Bulletin of Faculty of Science, Zagazig University (BFSZU)
e-ISSN: 1110-1555
Volume-2025, Issue-4, pp-115-125
https://bfszu.journals.ekb.eg/journal
Research Paper DOI: **10.21608/bfszu.2025.368006.1492**

==========

The impact of the negative velocity feedback controller on a generator of a hybrid electric vehicle subject to external force

Y. A. amer[1], A.T. EL-Sayed [2,] Taher A. Bahnasy[3], and Fatma. Sh. Mohammed[٤]

[1]*Department of Mathematics, Faculty of Science, Zagazig University, Zagazig, Egypt* yaamer@zu.edu.eg
[2]Department of basic science، Modern academy for Engineering and technology, Cairo, Egypt; atelsayed@eng.modern-academy.edu.eg
[3]Physics and Engineering Mathematics Dep., Faculty of Engineering, Tanta University, Tanta, Egypttaher.bahnasy@f-eng.tanta.edu.eg
[٤]Higher Institute of Engineering and Technology, fifth settlement fatemasherif1997@gmail.com

***ABSTRACT*: This purpose of this paper is to determine the stability domain of the powertrain of hybrid electric vehicles under different drive mode with multiple excitation sources, such as irregular internal excitation (engine and motor), external excitation (road) which can result in shaft failure. The multiple scale technique (MSPT) is used to develop and solve the simplified two-mass nonlinear dynamic model of second order for the hybrid elective vehicles powertrain (HEVP) in order to produce an approximate solution. HEVP is studied on the existence of external force at super harmonic resonance case ($\omega_0 \cong 2\omega$). The negative velocity feedback control (NVF) is used to control the amplitude of HEVP vibration. The mathematically derived frequency response equation is used in the numerical solutions that obtained using Rung-Kutta procedure. Comprehensive comparison of the amplitudes is served by using the time history program before and after the control of NVF. Response curves for frequency (angular speed) were studied at specific system coefficients that were both controlled and uncontrolled. The influence of various system parameters on the stability behavior are discussed.**

KEYWORDS:* *Hybrid electric vehicle powertrain - Negative velocity feedback - Multiple scale technique - Time history – Frequency response

---

Date of Submission: 13-03-2025 Date of acceptance: 22-04-2025

I. INTRODUCTION

Over the past few years, vehicle electrification has become an increasingly popular solution to the issues of air pollution and the depletion of non-renewable energy sources associated with traditional fuel-powered cars. Series hybrid electric vehicle powertrain (SHEVP) is powered by two or more energy sources, such as thermal and electric power. SHEVP can be categorized into three basic architectures: parallel, series, and series-parallel, depending on how the energy sources are connected to the powertrain. In a series SHEV, the engine connects to a permanent magnet synchronous motor (PMSM) but there is no connection between the internal combustion engine and the powertrain. in parallel SHEV, the electric motor and internal combustion engine are mechanically connected to the powertrain [1,2]. It is important to note that an unbalanced distribution of power between these sources can result in significant vibrations in the rotor, which can lead to instability in the entire transmission system [3, 4]. The HEV powertrain is a multi- Degree of freedom (DOF) nonlinear system with several excitation sources. Tang et al. [5], developed a 16-DOF torsional vibration model for the HEV power system. Chen et al. [6], developed the electromechanical coupling-based two-mass torsional vibration model of a HEV powertrain. A mathematical model for explaining the vibrations seen in PMSM and a demonstration of the parameters space in which a chaotic attractor emerges are introduced by Xue et al. [7]. Chen et al. [8, 9] investigated the nonlinear electromagnetic torque in the PMSM using electromagnetic theory to look at how the torsion angle affected on the angle between the stator and the magnetic motive force. Rotating machinery can experience torsional vibration, which is an undesirable phenomenon because, if left unchecked, it can harm and occasionally destroy other machines and structures [10]. The goal of current research is to eliminate or significantly lower the vibration risk in mechanical systems Vibration can be reduced with a variety of controller types, including passive, semi-active, and active control. Using mathematical methods to analyze and

predict possible vibration issues and their resolution is an important part of mechanical vibration analysis. Pei-Ming et al. [11], illustrated that the most effective tools for passive vibration control is the dynamic absorber, which can gather the vibration systems. Authors in [12-15] claimed the passive control organization is a common technique to settle down and control key vibration systems. ElSayed et al. [16] investigated the nonlinear pendulum system's vibration and stability while employing passive control to describe a ship's roll motion. El-Bassiouny and Eissa [17] used nonlinear mechanical oscillator that was being simulated by external and resonant parametric inputs by applying the multiple time scale approach.

The pivot motion of a simple pendulum with a stiff arm fastened to a longitudinal absorber and moving on an elliptical route was examined by L. Lautsch and T. Richter [18]. They succeeded in decoupling the rapid and sluggish scales by introducing regional averages and substituting localized periodic-in-time issues for rapid scale inputs. They were able to develop a posteriori error estimator by using the dual-weighted residual technique and segmenting errors into averaging error, slow scale error, and rapid scale error. The authors showed how to apply the error estimator for adaptive control of a numerical MSPT and confirmed its correctness. M. Kovaleva et al. [19] examined the stationary and nonstationary oscillation behavior of a parametric pendulum using the concept of restricted phase trajectories. A simpler model that might be able to predict highly modulated patterns outside of the typical range of beginning circumstances was proposed. T. S. Amer et al. [20], the authors investigate how a piezoelectric device affects a dynamical system with two degrees of freedom. Lagrange's equations are used to create the governing system of equations of motion, and the MSP and 4-RK methods are used to produce approximate and numerical solution, respectively. After removing secular elements, resonance cases are classified, and the solvability criteria are determined. The energy collecting device's outputs are examined and the ME for two scenarios is investigated. T. S. Amer et al. [21], look at a 3DOF dynamical system using an electromagnetic harvesting device and a magnet. The system's equations of motion are derived from Lagrange's equations and are then analytically solved with the MSP. To determine areas of stability and instability, apply the Routh-Hurwitz criterion. A displacement-velocity feedback control mechanism is proposed by C. Cheng et al. [22] to enhance the isolating performance of the quasi-zero stiffness vibration isolations (QZSVI). Time delay is considered in the electronically regulated QZSVI system. The way to further enhance the QZSVI for superior overall performance are described by Ch. Liu et al. [23]. Moreover, several instances of QZSVI's technical applications are given. The dynamic model is constructed using the Lagrange equation, according to H. Pu et al. [24]. New indicators of the QZSVI are then created and compared with other isolators, as well as the width of the QZSVI region and the linearity of stiffness. An experimental platform is then set up to verify the theoretical outcomes.

The vibration characteristics of a motor rotor were examined by Amer et al. [25], along with the impact of speed controllers and electro-mechanical couplers with multiple excitation forces. In the worst-case scenario of resonance, they discovered that the velocity feedback controller works better for this system when external and parametric excitation forces are present. Y. S. Amer and Taher A. Bahnasy [26] provided clarification and assess an externally stimulated Duffing oscillator under feedback control under the worst resonance scenario. For this system, the many time scales approach is used to obtain an analytical solution with both the existence and nonexistence of a time delay on the control loop. To lessen the amplitude peak, a suitable stability study is also carried out, and suitable options for the feedback gains and the time delay are discovered.

The aim of this research is to reduce vibrations caused by external forces in the main system using negative velocity feedback controller. The system time history is analyzed before and after the implementation of the controller using the fourth order Runge-Kutta method. The method of multiple scales is used to obtain an approximate solution up to the first approximation. The stability of the system is assessed under super harmonic resonance case. The system's behavior is simulated numerically with and without the negative velocity controller, the impact of selected coefficients is demonstrated through numerical data. A comparison between the numerical and analytical solutions was presented. The efficacy of various parameters and the device's behavior were illustrated using the MATLAB program.

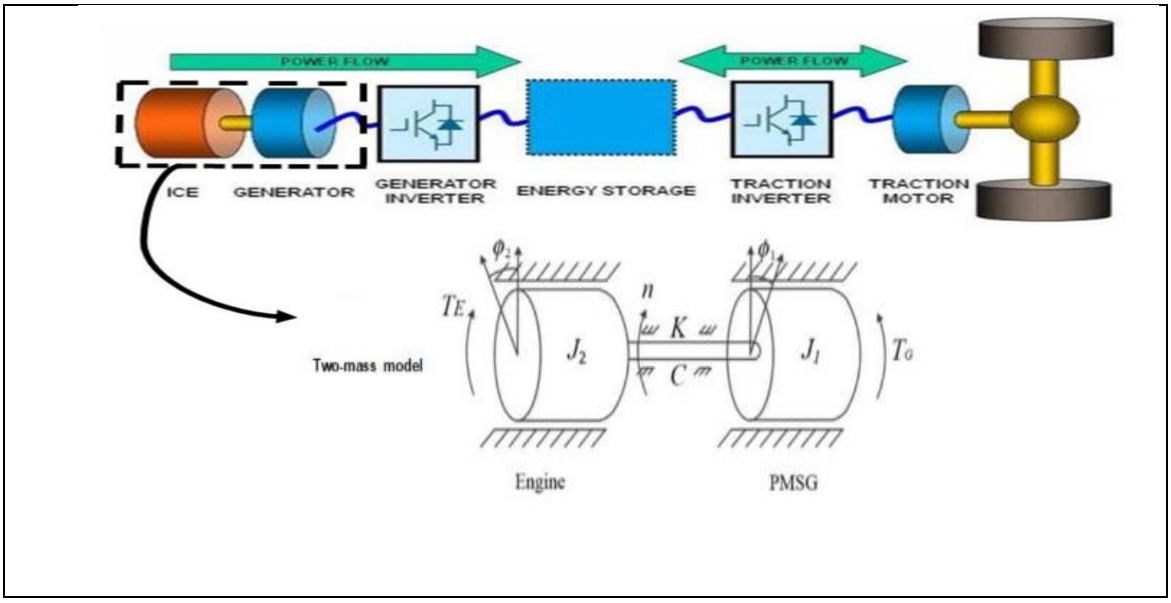

Figure 1: Diagram schematic and two-mass model of the power train of a series hybrid electric vehicle [27].

II.MATERIALS AND METHODS

The hybrid electric vehicle's schematic diagram as shown in Figure 1. Lagrange function [27] of the system is expressed in the following way:

$$L = \frac{1}{2} J_1 \dot{\phi}_1^2 + \frac{1}{2} J_2 \dot{\phi}_2^2 - \frac{1}{2} k (\phi_1 - \phi_2)^2 \quad (1)$$

Where ϕ_1 and ϕ_2 express the angle of the torsional vibration at the shaft's end. J_1, J_2 Called the moment of inertia, k is the stiffness of the equivalent shaft.
The expression representing the mechanical rotational equation of HEVP is given below:

$$\begin{aligned} J_1 \ddot{\phi}_1 + C(\dot{\phi}_1 - \dot{\phi}_2) + K(\phi_1 - \phi_2) &= T_G \\ J_2 \ddot{\phi}_2 - C(\dot{\phi}_1 - \dot{\phi}_2) - K(\phi_1 - \phi_2) &= -T_E \end{aligned} \quad (2)$$

Where T_{G_0} And T_{E_0} are the component of engine and which electromagnetic torque which are constant. The following represents the torsional vibration angle ϕ_j

$$\begin{aligned} &\phi_1 = \phi_1^{(o)} + \theta_1 \,, \phi_2 = \phi_2^{(o)} + \theta_2 \,, \\ &\dot{\phi}_1^{(o)} = \ddot{\phi}_1^{(o)} \,, \dot{\phi}_2^{(o)} = \ddot{\phi}_2^{(o)} \,, \end{aligned} \quad (3)$$

Where $\phi_j^{(o)}$ represent torsional angle between the PMSG and the engine, θ_i are torsional vibration angle at the end of the equivalent shaft.
Below are the corresponding equations that describe the torsional vibration of the powertrain in HEVP when subjected to disturbance in electromagnetic torque ΔT_G and load torque ΔT_E .

$$\begin{aligned} &J_1 \ddot{\theta}_1 + C(\dot{\theta}_1 - \dot{\theta}_2) + K(\theta_1 - \theta_2) = \Delta T_G \,, \\ &J_2 \ddot{\theta}_2 - C(\dot{\theta}_1 - \dot{\theta}_2) - K(\theta_1 - \theta_2) = -\Delta T_E \,, \end{aligned} \quad (4)$$

We substitute the following equation into Equations (4): $\Delta T_G = k_1\theta_1 - k_2\theta_2 - k_3\theta_3 - k_4\theta_4 - k_5\theta_5$, $\Delta T_M = F\sin(2\omega t)$ and considering the new variable $x = \phi_1 - \phi_2$ .For a series hybrid electric vehicle, we drive mathematical model of the torsional vibration as follow :

$$\ddot{x} + \mu\dot{x} + \alpha x + \eta x^2 + \beta x^3 + \varsigma x^4 + \gamma x^5 = F\sin(2\omega t) \quad (5)$$

Where:

$$\mu = c(\frac{1}{J_1}+\frac{1}{J_2}), \alpha = k(\frac{1}{J_1}+\frac{1}{J_2}) - k_1, \eta = \frac{k_2 r^2}{J_1}, \beta = \frac{k_3 r^3}{J_1}, \varsigma = -\frac{k_4 r^4}{J_1}, \gamma = \frac{k_5 r^5}{J_1}, F = \frac{F}{J_1}, r = \frac{1}{1+\nu}, \nu = \frac{J_1}{J_2},$$

We shall examine the case in which this symmetry is not broken in order to determine the potential energy function. Specifically, we set $\varsigma = \eta = 0$.

Then the mathematical model of the system without any control represented as:

$$\ddot{x} + \omega_0^2 x + \mu \dot{x} + \beta x^3 + \gamma x^5 = F \sin(2\omega t) \quad (6)$$

Perturbation technique

Modeling the system mathematically with a velocity feedback controller will be:

$$\ddot{x} + \omega_0^2 x + \varepsilon(\mu \dot{x} + \beta x^3 + \gamma x^5) = F \sin(2\omega t) - \varepsilon k \dot{x}(t) \quad (7)$$

Where ($\hat{\mu} = \varepsilon\mu, \hat{\beta} = \varepsilon\beta, \hat{\gamma} = \varepsilon\gamma$).

Applying the concept of multiple scale perturbation technique MSPT [28] as follows:

$$x(t:\varepsilon) = x_o(T_o, T_1) + \varepsilon x_1(T_o, T_1) + O(\varepsilon^2) \quad (8)$$

Where ε is a small dimensionless parameter of the perturbation and $0 < \varepsilon \le 1$, $T_o = t$ and $T_1 = \varepsilon t$ are the fast and slow time scale respectively the derivatives operator can be defined as

$$\frac{d}{dt} = D_0 + \varepsilon D_1, \qquad \frac{d^2}{dt^2} = D_0^2 + 2\varepsilon D_0 D_1, \quad D_j = \frac{\delta}{\delta T_j} (j = 0,1) \quad (9)$$

Substituting Equation (8), and (9) into (7) and equating the coefficient of same power of ε we obtain the following differential equations:

$O(\varepsilon^0)$:

$$(D_0^2 + \omega_0^2) x_0 = 0 \quad (10)$$

$O(\varepsilon^1)$:

$$(D_0^2 + \omega_0^2) x_1 = -2D_0 D_1 x_0 - \mu D_0 x_0 - \beta x_0^3 - \gamma x_0^5 + F \sin(2\omega t) - k D_0 X_0 \quad (11)$$

The general solution of Equation (10) is

$$x_0 = A e^{i\omega_0 T_0} + \overline{A} e^{-i\omega_0 T_0} \quad (12)$$

Substituting Equation (12) into (11), we obtain:

$$(D_0^2 + \omega_0^2) x_1 = (-2i\omega_0 D_1 A - i\mu\omega_0 A - 3\beta A^2 \overline{A} - 10\gamma A^3 \overline{A}^2 - ik\omega_0 A) e^{i\omega_0 T_0}$$
$$-(\beta A^3 + 5\gamma A^4 \overline{A}) e^{3i\omega_0 T_0} - \gamma A^5 e^{5i\omega_0 T_0} - \frac{iF}{2} e^{2i\omega t} + cc. \quad (13)$$

Where cc. refers to the complex conjugate of the existing terms. We will study the system amplitude at resonance case i.e. $2\omega = \omega_0 + \varepsilon\sigma$. Now Equation (13) will be:

$$(D_0^2 + \omega_0^2) x_1 = (-2i\omega_0 D_1 A - i\mu\omega_0 A - 3\beta A^2 \overline{A} - 10\gamma A^3 \overline{A}^2 - ik\omega_0 A) e^{i\omega_0 T_0}$$
$$-(\beta A^3 + 5\gamma A^4 \overline{A}) e^{3i\omega_0 T_0} - \gamma A^5 e^{5i\omega_0 T_0} - \frac{iF}{2} e^{i\omega_0 t + i\sigma T_1} + cc \quad (14)$$

Neglecting all the secular term in equation (14), then we get:

$$-2i\omega_0 D_1 A - i\mu\omega_0 A - 3\beta A^2 \overline{A} - 10\gamma A^3 \overline{A}^2 - ik\omega_0 A - \frac{iF}{2} e^{i\sigma T_1} = 0 \quad (15)$$

Converting $A = \frac{1}{2} a e^{i\phi}$ in polar form where a , and ϕ are both function of T_1,

$D_1 A = (i\dot{\phi} a + \dot{a}) \frac{e^{i\phi}}{2}$, then equation (15) will be in the form:

$$-i\omega_0 (i\dot{\phi} a + \dot{a}) e^{i\phi} - \frac{i\mu\omega_0 a}{2} e^{i\phi} - \frac{3\beta a^3}{8} e^{i\phi} - \frac{5a^5\gamma}{16} e^{i\phi}$$
$$-\frac{iF}{2} e^{i\sigma T_1} - ik\omega_0 \frac{a}{2} e^{i\phi} = 0 \quad (16)$$

Dividing by $e^{i\phi}$ and let $\theta = \sigma T_1 - \phi$, hence:

$$\omega_0 \dot{\phi}\, a - i\,\omega_0 \dot{a} - \frac{i\,\mu\omega_0 a}{2} - \frac{3\beta a^3}{8} - \frac{5a^5\gamma}{16} - \frac{iF}{2}(\cos(\theta) + i\,\sin(\theta)) - \frac{ika\omega_0}{2} = 0 \quad (17)$$

Equating the imaginary and the real part in equation (17) we obtain:

$$\dot{a} = \frac{-\mu a}{2} - \frac{ka}{2} - \frac{F}{2\omega_0}\cos(\theta) \quad (18)$$

$$a\dot{\theta} = a\sigma - \frac{3\beta a^3}{8\omega_0} - \frac{5a^5\gamma}{16\omega_0} + \frac{F}{2\omega_0}\sin(\theta) \quad (19)$$

Equilibrium solution

To obtain the steady state solution, let $\dot{a} = 0$ and $a\dot{\theta} = 0$ into equations (18) and (19), squaring the resultant formulas and adding to have the frequency response equation as follows:

$$(\frac{25\gamma^2}{256\omega_0^2})a^{10} + (\frac{15\beta\gamma}{64\omega_0^2})a^8 + (\frac{9\beta^2}{64\omega_0^2} - \frac{5\sigma\gamma}{8\omega_0})a^6 - (\frac{3\beta\sigma}{4\omega_0})a^4 \quad (20)$$
$$+(\frac{\mu^2}{4} + \frac{\mu k}{2} + \frac{k^2}{4} + \sigma^2)a^2 - (\frac{f^2}{4\omega_0^2}) = 0$$

In order to talk about how these solutions behave when they are stable, linearizing equations (18) and (19) to give the following system:

$$\begin{bmatrix}\dot{a}\\ \dot{\theta}\end{bmatrix} = J\begin{bmatrix}a\\ \theta\end{bmatrix} \quad (21)$$

where:

$$J = \begin{bmatrix}J_{11} & J_{12}\\ J_{21} & J_{22}\end{bmatrix} = \begin{bmatrix}\frac{\partial\dot{a}}{\partial a} & \frac{\partial\dot{a}}{\partial\theta}\\ \frac{\partial\dot{\theta}}{\partial a} & \frac{\partial\dot{\theta}}{\partial\theta}\end{bmatrix}, \text{ is the Jacobin matrix} \quad (22)$$

Where:

$$J_{11} = \frac{\partial\dot{a}}{\partial a} = \frac{\mu - k}{2},$$
$$J_{12} = \frac{\partial\dot{a}}{\partial\theta_1} = \frac{F}{2\omega_0}\sin(\theta), \quad (23)$$
$$J_{21} = \frac{\partial\theta}{\partial a} = \frac{\sigma}{a} - \frac{9\beta a}{8\omega_0} - \frac{25\gamma a^3}{16\omega_0},$$
$$J_{22} = \frac{\partial\dot{\theta}}{\partial\theta} = \frac{F\cos(\theta)}{2\omega_0 a}$$

The stability of the steady-state solution based on the eigenvalues of the Jacobin matrix which can be obtained by:

$$\begin{vmatrix}J_{11} - \lambda & J_{12}\\ J_{21} & J_{22} - \lambda\end{vmatrix} = 0 \quad (24)$$

Equation (40) can be written in the form:

$$\lambda^2 + H_1\lambda + H_2 = 0 \quad (25)$$

where:

$$H_1 = -(J_{11} + J_{22}),$$
$$H_2 = J_{11}J_{22} - J_{12}J_{21}. \quad (26)$$

For the above system's solution to be stable, the Routh-Huriwitz criterion must be satisfied such that: $H_1 > 0,$ and $H_2 > 0$. These conditions are satisfied numerically with the help of MATLAB code.

I. RESULTS AND DISCUSSION

Numerical consequence:

We used the "Ode 45" package in the MATLAB program [29] to quantitatively examine the system`s results. Also, we investigate the stability of the system using the multiple scale technique and the effects of various parameter on the behavior of the controlled system were demonstrated. We offered the comparison between the

approximate solution which obtained by multiple scale method and the numerical. The basic parameters are selected as the following: $\mu = 0.01,\ \gamma = 0.5,\ \beta = 0.005,\ \omega_0 = 10\ , \omega = 5, F = 150, k = 10$.

Time history

The behavior of the system is studied at super harmonic resonance case before and after using the linear velocity feedback control. Figure 2 (a) and (b) display the time history and phase plane of the main system before control. Figure 3 (a) and (b) illustrate the time history and phase plane of the main system after control ($k = 10$) at super harmonic resonance case. Figure 4 (a) and (b) show that the Poincaré mapping before and after control. where Figure 5 (a) and (b) shows a comparison of the approximate and the numerical solution that obtained by MST and RK-4 respectively .From these figures, it displays that the time history of the system without control has amplitude 7.532, and 1.363 when the system was given an negative velocity feedback controller, so effectiveness of the control (E_a = amplitude of uncontrolled system -amplitude of controlled system/ amplitude of uncontrolled system) about 82%. These figures also showed how numerical solution and approximate solution using multiple scale method agreed.

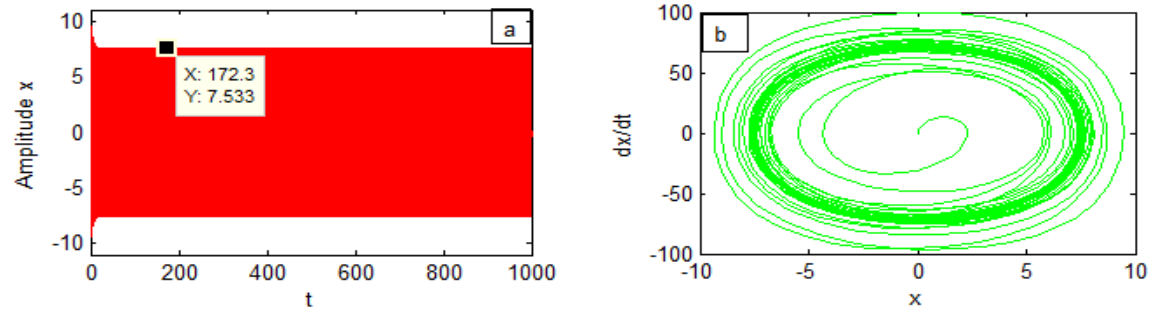

Figure 2: The main system amplitude (a) without control at resonance case $\omega_0 = 10\ , \omega = 5$ and (b) phase plane

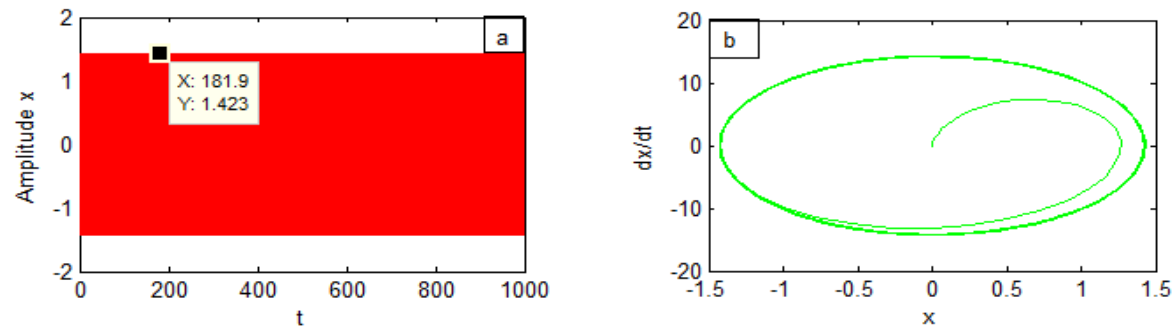

Figure 3: The main system amplitude (a) with control $k = 10$ at resonance case $\omega_0 = 10\ , \omega = 5$ and (b) phase plane.

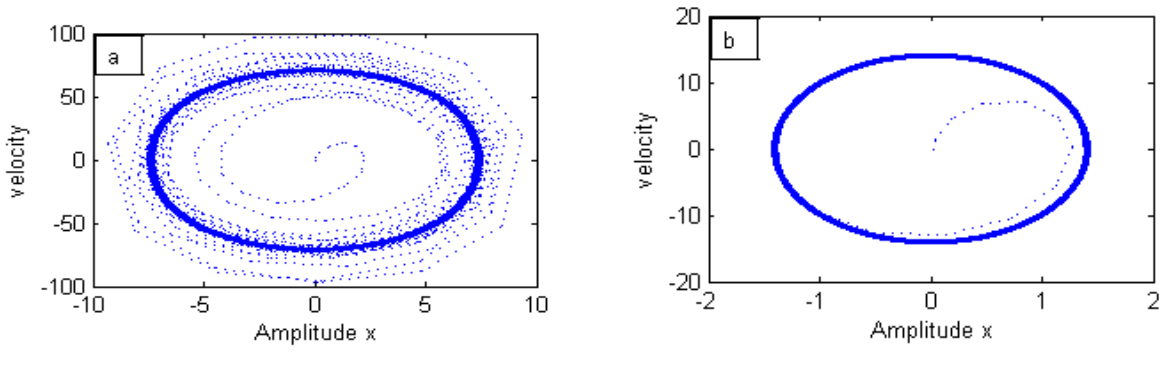

Figure 4: The Poincaré mapping at resonance case $\omega_0 = 10$, $\omega = 5$, (a) without control and (b) with control.

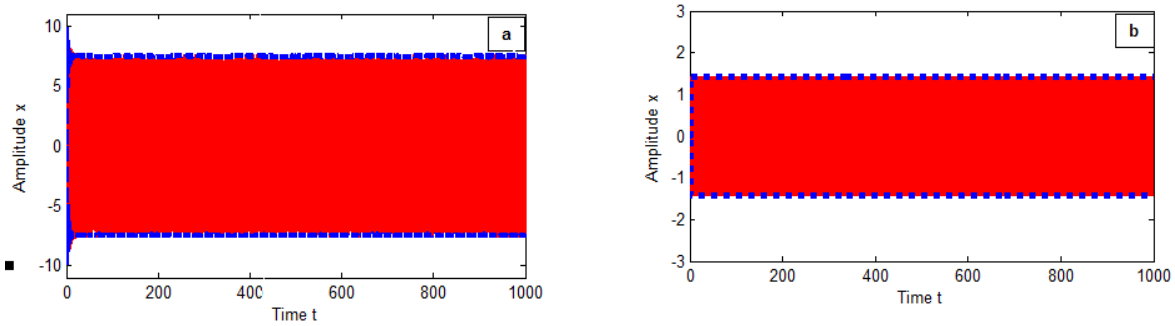

Figure 5: Comparison of time history of the system between the numerical solution and the approximate solution with (a) k=0 and (b) k=10.

Frequency response

In this section, we explain the frequency response curve and the effects of some parameters, from the Figure 6 (a), we can observe that the amplitude are shifted to the left with the increase of β , and Figure 6 (b) The amplitude of the controlled system are reduced by increasing the value of natural frequency ω . One can observe that the amplitude is inversely proportional to damping coefficient μ ,and directly proportional to the excitation force f as shown on Figure 7 (a) and (b) respectively. From Figure 8, we can observe that the amplitude is inversely proportional to the nonlinear term coefficient and the controller gain factor k . Figure 9. Represent the frequency response of the system with negative velocity feedback control.

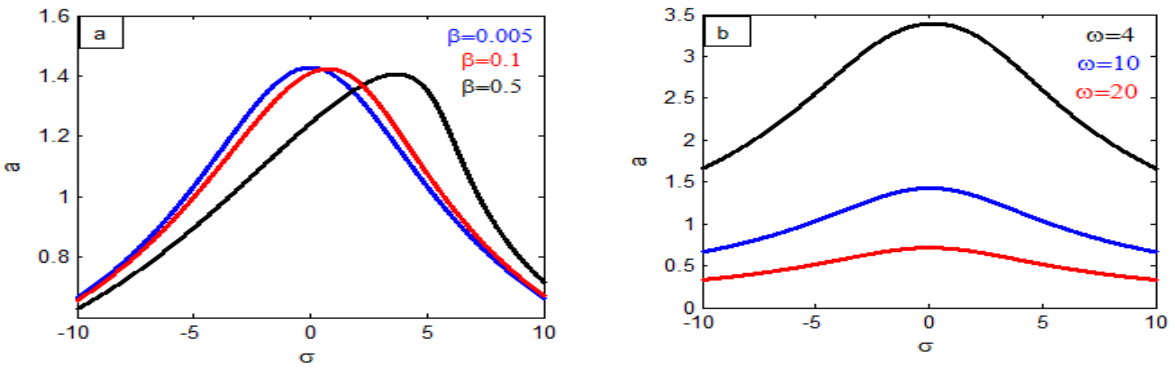

Figure 6: (a) The effectiveness of β at different values and (b) the effective of natural frequency ω .

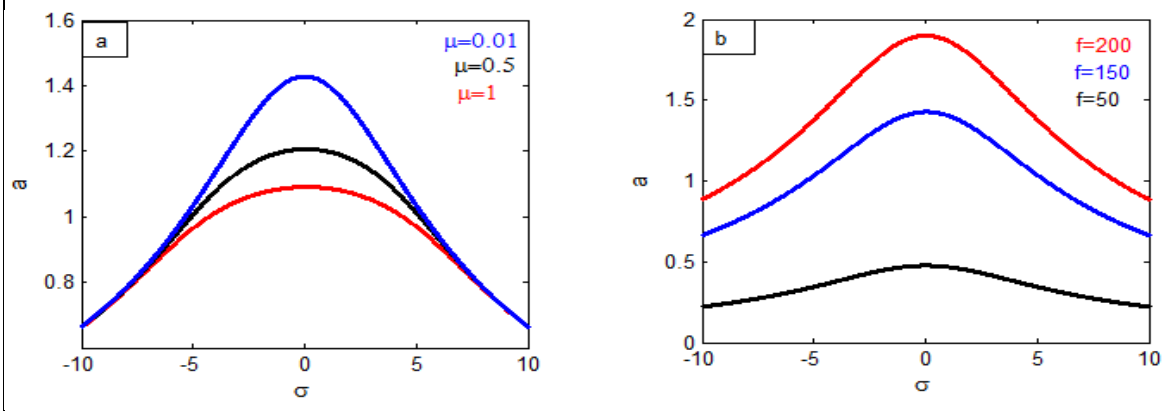

Figure 7:(a) The effectiveness of damping parameter μ at different values, and (b) the effectiveness of external force f at different values.

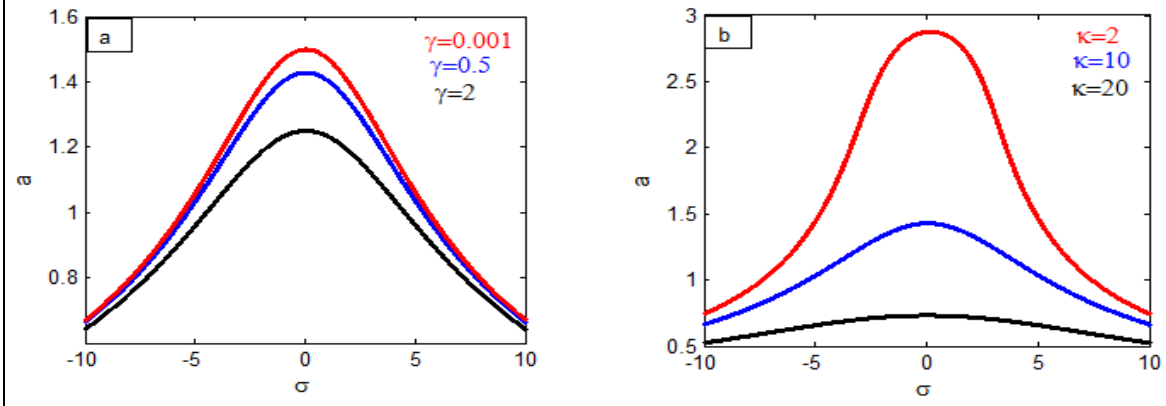

Figure 8: (a) The effectiveness of the γ parameter at different value and (b) the effectiveness of control k at different parameter

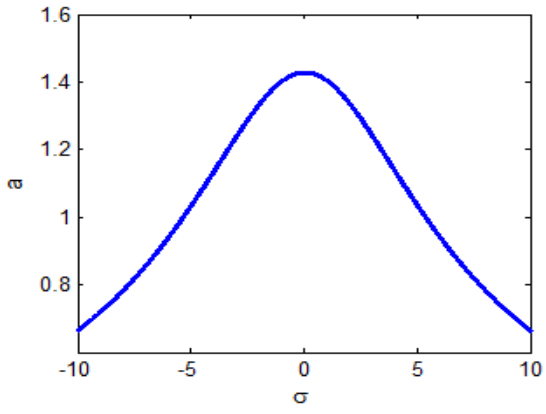

Figure 9: The response curve of the main system with Negative velocity feedback controller

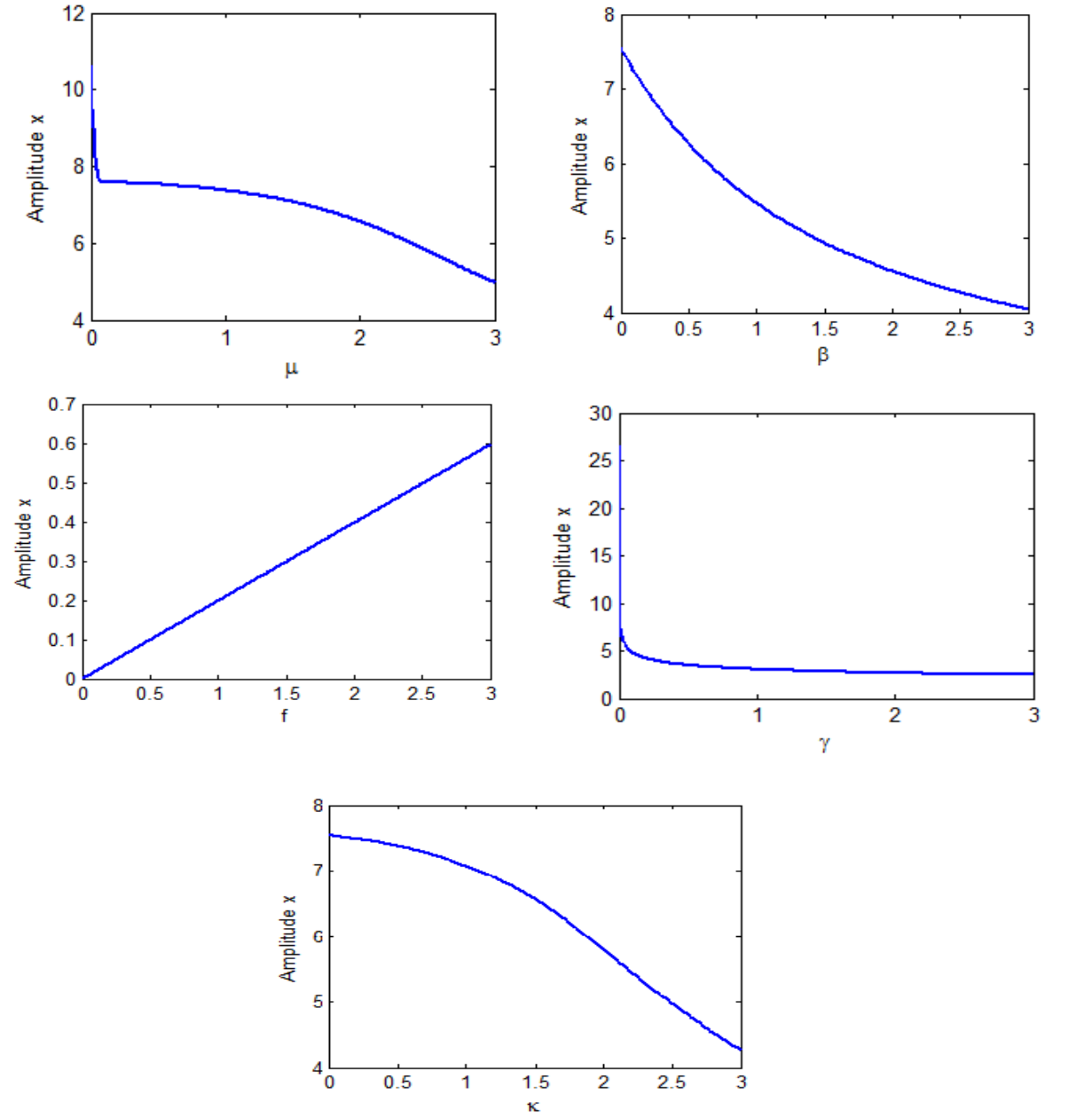

Figure 10: The effects of the parameters of the main system on the amplitude at $k = 0$.

The effect of various parameter on the main system without control is shown in Figure10. We can note that the amplitude of the system is monotonic decreasing when the damping coefficient μ , nonlinearities coefficient β , and γ are increasing, but while the increase of the external force, the amplitude of the main system is increasing, so that the system must be controlled. In addition, the amplitude of the main system is monotonically declining with a rise of the controller gain coefficient k .

Conclusion

The vibration system of the hybrid electric vehicle is controlled in this paper by using the active control, which applied to reduce the vibration through negative velocity feedback (NVF).the equation of the motion of this system contains quadratic and cubic nonlinearities .The multiple scale technique (MST) is utilized to determine an approximate solution for the ordinary differential equation represented this system at worse case

(super harmonic resonance case($2\omega \cong \omega_o$).the stability of the obtained numerical solution is investigated using response curve equation .the effect of different parameter on the vibrating system are investigated .from the above study ,we can list the following results:

(1) The super harmonic resonance case ($2\omega \cong \omega_o$) is the worst resonance case of the vibration system.
(2) After using negative velocity feed-back the amplitude of the vibration system was reduced by about 82% from without control.
(3) The effectiveness of negative velocity feedback E_a is about 6.
(4) The behavior of the controlled system increased with increasing the negative velocity coefficient k.
(5) With an increase in the damping coefficient, the controlled system's behavior decreased.

List of abbreviations and symbols

MSPT	Multiple time scale perturbation technique
FR	Frequency response
HEVP	Hybrid elective vehicles powertrain
RK-4	The fourth-order Runge-Kutta procedure
ω_0	Natural frequency of the system
μ	Damping coefficients
β, γ	Nonlinear terms coefficients
k	Controller feedback gain
ε	Small perturbation parameter
cc	Complex conjugate
PR	Primary resonance
SR	Simultaneous resonance
SHEVP	Series hybrid electric vehicle powertrain
PMSM	Permanent magnet synchronous motor
DOF	Degree of freedom
QZSVI	Quasi-zero stiffness vibration isolations

References

[1] Wang, H., Huang, Y., and Khajepour, A., Cyber-physical control for energy management of off-road vehicles with hybrid energy storage systems, *IEEE/ASME transactions on mechatronics*, *23*(6), 2609-2618. (2018)

[2] Guo, H., Wang, X., and Li, L., State-of-charge-constraint-based energy management strategy of plug-in hybrid electric vehicle with bus route, *Energy Conversion and Management*, *199*, 111972. (2019).

[3] Calleecharan, Y., and Aidanpää, J. O., Stability analysis of an hydropower generator subjected to unbalanced magnetic pull, *IET science, measurement & technology*, *5*(6), 231-243. (2011)

[4] Abdalaziz, M., Sedaghati, R., and Vatandoost, R., Design optimization and experimental evaluation of a large capacity magnetorheological damper with annular and radial fluid gaps, *Journal of Intelligent Material Systems and Structures*, 34(14), 1646-1663. (2023)

[5] Tang, X., Jin, Y., Zhang, J., Zou, L., and Yu, H., Torsional vibration and acoustic noise analysis of a compound planetary power-split hybrid electric vehicle, *Proceedings of the Institution of Mechanical Engineers, Part D: Journal of Automobile Engineering*, *228*(1), 94-103. (2014).

[6] Chen, K., Hu, J., and Peng, Z., Analysis of Active Vibration for HEVs through electro-mechanical coupling, *Energy Procedia*, *105*, 3164-3172. (2017).

[7] W. Xue, Y. L. Guo, and Y. L. Li, Chaos Characteristics and Control of Permanent Magnet Synchronous Motors, *Journal of Applied Mechanics and Materials*, Vol. 48-49, 292-299. (2011).

[8] Chen, X., Hu, J., Peng, Z., & Yuan, C., Bifurcation and chaos analysis of torsional vibration in a PMSM-based driven system considering electromechanically coupled effect, *Journal of Nonlinear Dynamics*, *88*, 277-292. (2017).

[9] Chen, X., Yuan, S., & Peng, Z., Nonlinear vibration for PMSM used in HEV considering mechanical and magnetic coupling effects, *Nonlinear Dynamics*, *80*, 541-552. (2015).

[10] E. Abouobaia, R. Bhat, and R. Sedaghati, Development of a new torsional vibration damper incorporating conventional centrifugal pendulum absorber and magnetorheological damper, Journal of Intelligent Material Systems and Structures, 27(7),1-13. (2015).

[11] S. Pei-ming, L. Ji-zhao, J. Jin-shui, L. Bin and H. Dong-ying ,Nonlinear dynamics of torsional vibration for rolling mill's main drive system under parametric excitation, Journal of Iron and Steel Research, 20 (1), 7-12. (2013).
[12] A. H. Nayfeh and D. T. Mook, Nonlinear Oscillations, New York, *John Wiley*, (1979)
[13] D. J. Mead, Passive Vibration Control, England, *John Wiley & Sons*, (1988).
[14] J. B. Hunt, Dynamic vibration Absorbers, London, *Mechanical Engineering Publications*, (1979).
[15] M. Eissa, Vibration control of non-linear mechanical system via a neutralizer, Electronic Engineering Bulletin for Faculty of Electronic Engineering Menouf , Egypt, 181-20. (1999).
[16] A. T. El-Sayed, M. Kamel and M. Eissa, Vibration reduction of a pitch roll ship model with longitudinal and transverse absorbers under multi excitations, *Mathematical and Computer Modelling*, 52, 1877-1898, (2010).
[17] A. F. El-Bassiouny and M. Eissa, Dynamics of a single-degree-of-freedom structure with quadratic, cubic and quartic non-linearities to a harmonic resonance, *Applied Mathematics and Computation*, 139, 1-21, (2003).
[18] L. Lautsch and T. Richter, Error estimation and adaptivity for differential equations with multiple scales in time, J. Comput. Methods Appl. Math. 21, 4, 841-861, (2021).
[19] M. Kovaleva, L. Manevitch, F. Romeo, Stationary and non-stationary oscillatory dynamics of the parametric pendulum, Comm. Nonlin. Sci. Num. Simul. 76, 1-11, (2019).
[20] T. S. Amer, T. A. Bahnasy, H. F. Abosheiaha, A. S. Elameer, A. Almahalawy, The stability analysis of a dynamical system equipped with a piezoelectric energy harvester device near resonance, J. Low Freq. Noise V. A., https://doi.org/10.1177/14613484241277308, (2024).
[21] T. S. Amer, A. Arab, A. A. Galal, On the influence of an energy harvesting device on a dynamical system, J. Low Freq. Noise V. A., 43(2), 669–705, (2024).
[22] C. Cheng, Y. Hu, R. Ma, W. Wang, Beneficial performance of a quasi-zero-stiffness vibration isolator with displacement-velocity feedback control, Nonlinear Dyn. 111, 6, 5165-5177, (2023).
[23] Ch. Liu, W. Zhang, K. Yu, T. Liu, Y. Zheng ,Quasi-zero-stiffness vibration isolation: Designs, improvements and applications, Eng. Struct. 301, 20240215, (2024).
[24] H. Pu, J. Liu, M. Wang, J. Ding, Y. Sun, Y. Peng, J. Luo ,Bio-inspired quasi-zero stiffness vibration isolator with quasilinear negative stiffness in full stoke, J. Sound Vib. 574, 20240331, (2024).
[25] Y. A. Amer, Taher A. Bahnasy, and Ashraf M. Elmhlawy, Vibration Analysis of Permanent Magnet Motor Rotor System in Shearer Semi-Direct Drive Cutting Unite with Speed Controller and Multi- Excitation Forces, Appl. Math. Inf. Sci. 15, No. 3, 373-381, (2021).
[26] Y. A. Amer, Taher A. Bahnasy, Duffing oscillator's vibration control under resonance with a negative velocity feedback control and time delay, Sound &Vibration, vol.55, no.3, 191-201, (2021)
[27] Tametang Meli, M. I., Leutcho, G. D., and Yemele, D., Multistability analysis and nonlinear vibration for generator set in series hybrid electric vehicle through electromechanical coupling, *Chaos: An Interdisciplinary Journal of Nonlinear Science*, *31*(7), 073126, 1-15., (2021).
[28] J. Kevorkian and J. D. Cole, Multiple Scale and Singular Perturbation Methods, *Applied Mathematical Sciences*, Springer-Verlag, first edition, (1996).
[29] R. V. Dukkipati, Solving vibration analysis problems using MATLAB, *New Age International Pvt Ltd Publishers*, (2007).